Multispectral radiometric characterization of coffee rust epidemic in different irrigation management systems

Miryan Silva de Oliveira Pires[a], Marcelo de Carvalho Alves[a,*], Edson Ampélio Pozza[b]

[a] Agricultural Engineering Departament, Federal University of Lavras, PO BOX 3037, CEP 37200-000, Lavras, MG, Brazil
[b] Plant Pathology Departament, Federal University of Lavras, PO BOX 3037, CEP 37200-000, Lavras, MG, Brazil

ABSTRACT

Coffee rust (*Hemileia vastatrix* Berk. & Br.) is one of the most prominent diseases in coffee (*Coffea arabica* L.) and causes serious damage to the crop. The pathogen incubation period may be long for about 30 days and 10% incidence of rust may result in 3 times more disease few days after the signals of rust appear in the leaves, even in the absence of new infections. The objective of this study was to evaluate the applicability of coffee crop monitoring under different irrigation systems by orbital radiometry, exploring the spectral signature and spectral, spatial and temporal pattern of rust incidence in the coffee field. The study was carried out in four areas of coffee plantations in Carmo do Rio Claro, Minas Geris, Brazil, between August 2012 and December 2014, under self-propelled, drip, center pivot irrigation systems and rainfed system. Fifteen Landsat-7/ETM + and Landsat-8/OLI-TIRS images were used, trying to establish a better sequence of images between *in situ* data of rust incidence in the coffee leaves and coffee leaf growth evaluated by sample meshes in the field along the time. Space-time disease incidence distribution maps, Pearson correlation and reflectance spectral signatures were used to evaluate coffee rust progress in the different irrigation fields. The highest coffee rust incidence occurred in August and corresponded to the values of lower NIR reflectance for all evaluated areas, independently of the irrigation management system. In the visible, SWIR-1 and SWIR-2 spectral regions, there were higher reflectance values in the rainfed area when compared to irrigated areas in rainy periods. There was a greater spectral and temporal variation of rust in the center pivot irrigation system when compared to the other irrigation management systems, presenting high values of average incidence of rust above 30% in the periods close to the harvest period, from June to August 2013 and 2014. The high incidence of rust associated with coffee fruit harvest probably led to a reduction in plant leaf growth in center pivot and rainfed fields. There was a negative correlation between near infrared and rust in the self-propelled and center pivot management systems. High coffee rust incidence values mainly in center pivot and rainfed coffee fields determined reduction in the average reflectance of NIR and green and increase reflectance in red, SWIR-1 and SWIR-2 when compared to periods with lower rust in the coffee fields.

1. Introduction

Coffee is a product consumed worldwide and has great importance in the Brazilian economy. Brazil is the largest producer of coffee in the world and the second largest consumer, and the state of Minas Gerais stands out as the largest producer (Ministério da Agricultura, 2016). Among the factors that affect coffee (*Coffea arabica* L.), coffee rust (*Hemileia vastatrix* Berk. Br.) is the most significant. This disease causes an intense reduction of leaf growth and reduction in productivity, and its intensity depends on the interaction between the environment, the host and the pathogen (Talamini et al., 2003; Agrios, 2005; Pozza et al., 2010). Another relevant factor in the production is the irrigation management, important to provide the adequate amount of water and avoid the water deficit whenever the rainfall is not sufficient to supply the water demand of the plant (Rodrigues et al., 2010). However, irrigation can alter the microclimate of the crop, modifying the environment conditions and increasing the period of leaf wetting (Rotem and Palti, 1969), which contributes to the increase of disease incidence (Carvalho and Chalfoun, 1999).

Accurate and timeous detection, mapping and monitoring of crop diseases and pests is critical for food security. Remote sensing can offer a viable method of obtaining critical crop information and levels of disease incidence, leaf growth and yield prediction due to its synoptic coverage, repetitiveness and cost-effectiveness. The physical principle

of remote sensing disease infected crops is based on changes in transpiration rate, chlorosis, leaf color, and morphology, which in turn affects plant spectral reflectance properties (Mutanga et al., 2017). Many researches about techniques of image processing and remote sensing used as support in the monitoring of plant diseases have been developed. Some examples of such diseases are the Asian soybean rust (Silva et al., 2009), corn leaf spot (*Cercospora zeae-maydis*) (Dhau et al., 2017), *Rizhoctonia solani* (Webb and Calderón, 2015), *Cercospora beticola, Erysiphe betae* e *Uromyces betae* (Mahlein et al., 2010) in beet, white mold (*Sclerotinea sclerotiorum*) in bean (Boechat et al., 2014), yellow rust (*Puccinia striiformis*) in wheat (Bravo et al., 2003), *Heterodera schachtii* and *Rhizoctonia solani* (Hillnhütter et al., 2012), *Magnaporthe grisea* (Kobayashi et al., 2001) in rice, *Phytophthora infestans* in tomato (Zhang et al., 2003) and *Venturia inaequalis* in apple trees (Delalieux et al., 2007).

In coffee crop, Chemura et al. (2016) evaluated the potential of the use of reflectance measurements to discriminate three levels of coffee rust severity (*Hemileia vastatrix*) in coffee leaves under greenhouse conditions. The Apogee VIS-NIR spectrometer with spectral range $400-900$ nm and spectral resolution of 0.5 nm was applied to simulate the Sentinel-2 satellite sensor bands. Katsuhama et al. (2018) used NDVI and standard deviation NDVI of Landsat 7 imagery to evaluate defoliation of coffee caused by coffee rust in Sierra Madre Mountains, Guatemala. The authors observed that rust progressed in-homogeneously inside a damaged area and the possibility to take early-stage countermeasures against the infection.

Monitoring diseases in coffee implies knowledge of flexible, multi-dimensional and multidisciplinary integrated management techniques to control diseases, employing biological, cultural, socioeconomic, physiographic and chemical measures necessary to keep diseases below the threshold of economic damage without harming the agroecosystem. For this, it is necessary to know sampling techniques and evaluate different resolutions that can potentially be used in disease monitoring. This step requires a lot of study because each researcher adopts a specific method and there may be questions about the size of the area and samples collected in the field. In cases where there is host leaf infection leading to signs of yellowing and wilting and causing defoliation of the plant, there may be a change in the host spectral characteristic regionalized in the field that can be detected remotely to establish proper management at the site where the disease manifests in the plant.

The knowledge about the host physiology on some epidemiological factors, such as latency and sporulation period is sufficient to known the rust epidemiology in order to predict its behaviour in different regions and to devise provisional chemical control schedules (Waller, 1982).

As there were studies indicating that coffee cultivation can be monitored by orbital sensors, and based on the hypothesis that moderate and high resolution radiometers can be applied in phases of the coffee production system, the objective was to evaluate the relation between the spectral radiometry of coffee plantations in different irrigation systems and the variables related to coffee rust, aiming to obtain spectral, spatial and temporal patterns of the disease progress from Landsat-7/ETM + and Landsat-8/OLI-TIRS imagery.

2. Material and methods

2.1. Study area

The study was carried out in four areas of coffee plantations located in Carmo, Rio Claro, Minas Gerais, Brazil, between August 2012 and December 2014.

Carmo do Rio Claro is located in the southwest region of the state of Minas Gerais and is bathed by Furnas Dam, with altitude of 798 m, latitude 20°58′17″ South and longitude 46°7′57″ West (Instituto Brasileiro de Geografia e Estatística (IBGE), 2010). The local climate is classified as subtropical mesothermic, according to the Köppen-Geiger

Table 1
Type of irrigation systems, size of area (ha), age of the crop (years), plant spacing (m. m $^{-1}$), density of the crop (plants. ha $^{-1}$).

Irrigation system	Area (ha)	Age (years)	Plant spacing (m. m $^{-1}$)	Density (plants. ha $^{-1}$)
Rainfed*	30	6	3.6 × 0.7	3968
Self-propelled	2.6	7	3.5 × 0.7	4081
Drip	11	2.5	3.6 × 0.7	3968
Center pivot	17	10	4.0 × 0.5	5000

 * Pruning in September 2013.

classification, and characterized by dry winters and wet summers (subtropical/tropical altitude - Cwa) (Kottek et al., 2006). According to the Climatological Normals of 1961–1990, the average winter temperature is approximately 16 °C, and the summer average is approximately 27 °C. The wettest period is between the months of December and February, and the driest is between April and September (Instituto Nacional De Meteorologia (INMET), 2016).

The coffee cultivated in the study areas is *Coffea arabica* L., cultivar Acaiá 474/19, managed by different irrigation systems (Table 1). Leaf miner and berry borer were chemically controlled, weeds were controlled by mowing. The coffee crops were fertilized according to the recommendations for managing soil fertility in the Minas Gerais state, Brazil, as proposed by Guimarães et al. (1999).

In general, irrigation was performed all year round according to the need of the plants, based on the measurement of tensiometers. Irrigation by center pivot started on June 2nd, 2012, with 30 mm applied every 10 days, watered to a monthly minimum depth of 90 mm, as monitored by a rain gauge. Irrigation by a drip system were irrigated throughout the year, based on readings from groups of tensiometers. Both experimental plots were not irrigated during harvest, from May to June.

The sampling points were georeferenced with GPS TRIMBLE 4600 LS® and Total Station TC600®. The rainfed, self-propelled, drip and center pivot areas had 51, 50, 52 and 50 sample points, respectively. Five plants were evaluated at each sampling point. The distance between sampling points ranged from 50 × 50 m, 30 × 30 m, 40 × 40 m and 40 × 40 m in the dry, self-propelled, drip and center pivot areas, respectively (Fig. 1).

2.2. In situ data

The *in situ* data collection of leaf growth and disease incidence was carried out in four coffee growing areas in Carmo do Rio Claro, approximately every two months during the period from August 2012 to December 2014.

2.2.1. Leaf growth

The leaf growth (%) was evaluated in the sample points according to the diagrammatic scale proposed by Boldini (2001), which consists of notes according to the percentage of leaf growth of the plants, for every 5 plants/point. These plants were marked for subsequent evaluations, which occurred every two months, from August 2012 to June 2014, totaling 12 evaluations.

The percentage of leaf growth was adapted from the classification by Boldini (2001), resulting in the null (0%), low (1–40%), moderate (40–70%) and high (> 70%) classes.

Average leaf growth curves of cultivated areas under self-propelled, drip, center pivot irrigation systems and rainfed system were determined for the evaluation periods from 2012 to 2014

2.2.2. Disease incidence

The disease incidence (%) was evaluated by sampling of 12 leaves per plant, by non-destructive method, in the middle third of the canopy, from the third and fourth leaves of the selected branch at random
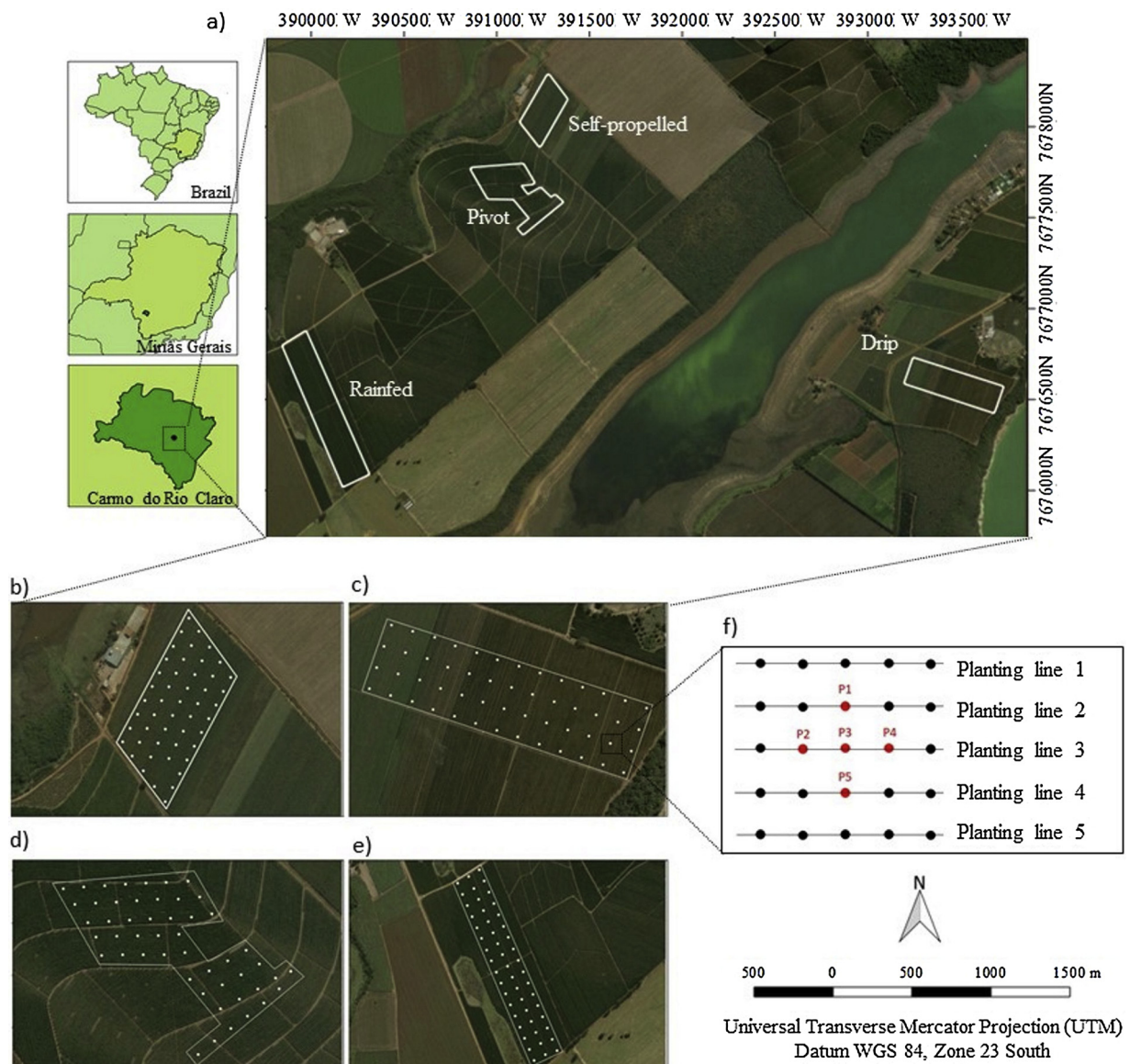
Fig. 1. Location map of coffee plantations in Carmo do Rio Claro, Minas Gerais, Brazil (a). Sampling meshes used to obtain *in situ* data as well as Landsat-7/ ETM + and Landsat-8/OLI-TIRS orbital images from areas under self-propelled, drip and center pivot irrigation systems and rainfed system (b, c, d and e) and sampling point with the location of the five plants sampled with reference in the planting lines (f).

(Huerta, 1963), such as 5 plants/sampling point, 12 leaves/plant, total of 60 leaves/sampling point. These plants were marked for subsequent evaluations, which occurred every two months from August 2012 to December 2014, totaling 15 evaluations.

The disease incidence was determined by percentage of leaves with symptoms in relation to the total sampled, according to Eq. 1 (Campbell and Madden, 1990):

$$I\ (\%) = (NFD\ /\ NFT) * 100 \tag{1}$$

where I (%) indicates the percentage of disease incidence, NFD is the number of diseased leaves and NFT is the number of leaves per treatment.

We used the distribution of all rust incidence evaluation values in all the irrigation fields to create incidence distribution classes by spatiotemporal symbol maps. The coffee rust incidence was classified into null (0%), low (1.00–16.67%), moderate (16.67–33.33%) and high (> 33.33%) for all evaluated coffee fields. Moderate rust incidence could be considered the time when control tactics should be employed to treat the disease, such as chemical control, irrigation techniques and

plant nutrition.

2.2.3. Disease progress curves

Based on the average incidence of all sampling points from each coffee field, disease progress curves were plotted over time for the evaluation periods from 2012 to 2014.

2.2.4. Climatic data

The climatic data were obtained *in situ* by a weather station from National Institute of Meteorology (INMET), installed in Lavras, MG, Brazil, about 120 km away from the study areas to monitor temperature and precipitation, being the one closest to the place of study and with data available for all dates. The mean temperature (˚C) and precipitation (mm) data were used for comparison criteria.

The monthly average of temperature and precipitation collected in the stations was plotted in graphs for criteria of comparison with the other variables of interest.

Table 2

Dates of *in situ* data and dates of LANDSAT-7/ETM + and LANDSAT-8/OLI-TIRS imagery collection.

In situ Data	LANDSAT-7 ETM + Imagery	LANDSAT-8 OLI/TIRS Imagery
08/15//2012	08/21/2012	
10/20/2012	10/08/2012	
11/27/2012	12/27/2012	
02/02/2013	02/13/2013	
04/17/2013	04/18/2013	
06/08/2013	05/20/2013	
08/24/2013	08/24/2013	
10/17/2013		11/04/2013
12/03/2013		11/20/2013
02/10/2014		02/08/2014
04/05/2014	04/05/2014	
06/04/2014	06/08/2014	
08/18/2014		08/19/2014
10/20/2014		10/22/2014
12/27/2014		12/25/2014

2.3. Remote sensing data

The study was developed using images from the LANDSAT-7/ ETM + and LANDSAT-8/OLI-TIRS satellites, obtained through a free download in the United States Geological Survey (USGS), regarding the date of each data collection *in situ*. Priority was given to cloud-free images and any interferences in the study area that could impair digital processing.

The images were chosen from two different sensors, because it was not possible to obtain only one of them, and the images were not suitable for use (*e.g.* clouds, shade) or had no proximity to the desired *in situ* date. For this reason, they were chosen so that they could be intercalated, forming sequence to favor the study of the areas.

The dates of the appropriate satellite images for the study and their dates of data collection *in situ* are presented in Table 2. The characteristics of Landsat-7/ETM + and Landsat-8/OLI-TIRS satellite sensors bands, spectral regions and spatial resolution were detailed in United States Geological Survey (USGS) (2016).

Radiometric climatic data obtained from MODIS time series provided by the National Institute for Space Research (INPE) was used to monitor temperature and precipitation in the evaluated coffee fields. The average temperature (°C) and precipitation (mm) data collected were used for comparison criteria. The monthly average of temperature and precipitation collected in the *in situ* stations was plotted in graphs for criteria of comparison with the other *in situ* studied variables.

2.3.1. Image processing

The methods used to extract the information from the images can be accessed in Albuquerque and Albuquerque (2000), as well as image processing techniques, stand out the radiometric correction, geometric and atmospheric in Vermote et al. (1997); Liu (2006); Marques Filho and Neto (1999); Florenzano (2011) and Tyagi and Bhosle (2014).

All satellite images and field boundaries of the studied areas have been reprojected to the Universal Transverse Mercator coordinate/WGS 84 (World Geodetic System), Zone 23 South. According to Crósta (1992), the satellite images are subject to geometric distortions, it is necessary to go through a pre-processing for data correction. It facilitates the use of image and derived products in geographic information systems (Jensen, 2009). The images obtained by the Higher-Level (Surface Reflectance) are already available with the atmospheric interference corrected by the Second Simulation of Satellite Signal in the Solar Spectrum (6S) method, which is based on the radiative transfer model (Vermote et al., 1997). The final result of the atmospheric correction is the denominated surface reflectance, being possible the spectral characterization of the objects present in the terrestrial surface (Ponzoni et al., 2012).

2.3.2. Spectral signature

To simplify the detection of disease by means of spectral sensors, different wavelengths can be used, since each disease influences the spectral signature in a characteristic way (Mahlein et al., 2013).

For the evaluation of the reflectance of coffee plantations were used the Blue (Green) and Red (Red) bands of the visible spectrum and the bands Infrared Near (NIR), Short-wave Infrared 1 (SWIR-1) and Short-wave Infrared 2 (SWIR-2) of the infrared spectrum.

The average reflectance of each band was calculated in the coffee fields and plotted in graphics of spectral reflectance in the evaluated periods.

2.3.3. Thermal infrared

The thermal infrared bands of Landsat-7 and Landsat-8 underwent a conversion of temperature values from Kelvin to Celsius.

The radiometric temperature values of each sample point were extracted using the mesh of points relative to each area of interest. From the obtained values, the graphs of average brightness values of temperature (°C) were elaborated.

2.4. Statistical analyzes

Pearson correlation coefficient values were obtained from the average reflectance of the blue, green, red, near infrared, short-wave infrared-1 and short-wave infrared-2 bands of Landsat-7 and Landsat-8 images and the average values of coffee rust incidence and leaf growth in all evaluation periods at each georeferenced point of each coffee area under self-propelled, drip, center pivot irrigation system and rainfed system.

3. Results

3.1. Spatial characterization

3.1.1. Coffee rust incidence

In the self-propelled irrigation system, the disease presented a low incidence (between 1.0 and 16.6%) in almost all evaluated months (Fig. 2), with a slight moderate increase in August and December 2013 (Fig. 2g and i) and areas with no incidence in October 2012 and May 2014 (Fig. 2b and k).

In the drip irrigation system, the disease presented null values, and when there were low incidence values, a greater disease progress was observed in August 2012 (Fig. 3a) and mainly from April to August (Fig. 3e, f and g). In June 2013 (Fig. 3f), the highest value of low average incidence of rust was registered among all the studied dates.

The center pivot irrigation system showed the highest variation in the disease progress when compared to the other evaluated treatments of irrigation and non-irrigation, presenting moderate to high incidence in the months close to harvest, in August of 2013 (Fig. 4g), June and August 2014 (Fig. 4l and m), and months with near zero incidence, almost always in October 2012 (Fig. 4b) and April 2014 (Fig. 4k).

In the rainfed system, the months with moderate to high disease spatial progress were in June 2013 (Fig. 5f) and August 2013 (Fig. 5g). The disease appeared with low incidence in all field extent mainly in the months of August, November 2012, February, April, June 2013 and June, August, December 2014 (Fig. 5).

3.1.2. Leaf growth

In the area under self-propelled irrigation, the percentage of leaf was moderate mainly in August and October 2013 (Fig. 6g and h) and June 2014 (Fig. 6l). In the other periods, the leaf growth was high in all field extent (Fig. 6)

In the area cultivated under a drip irrigation system, the leaf growth was high in all the periods, except in August, December 2013 and April, June 2014, with moderate values (Fig. 7).

In the area under center pivot irrigation, the percentage of leaf
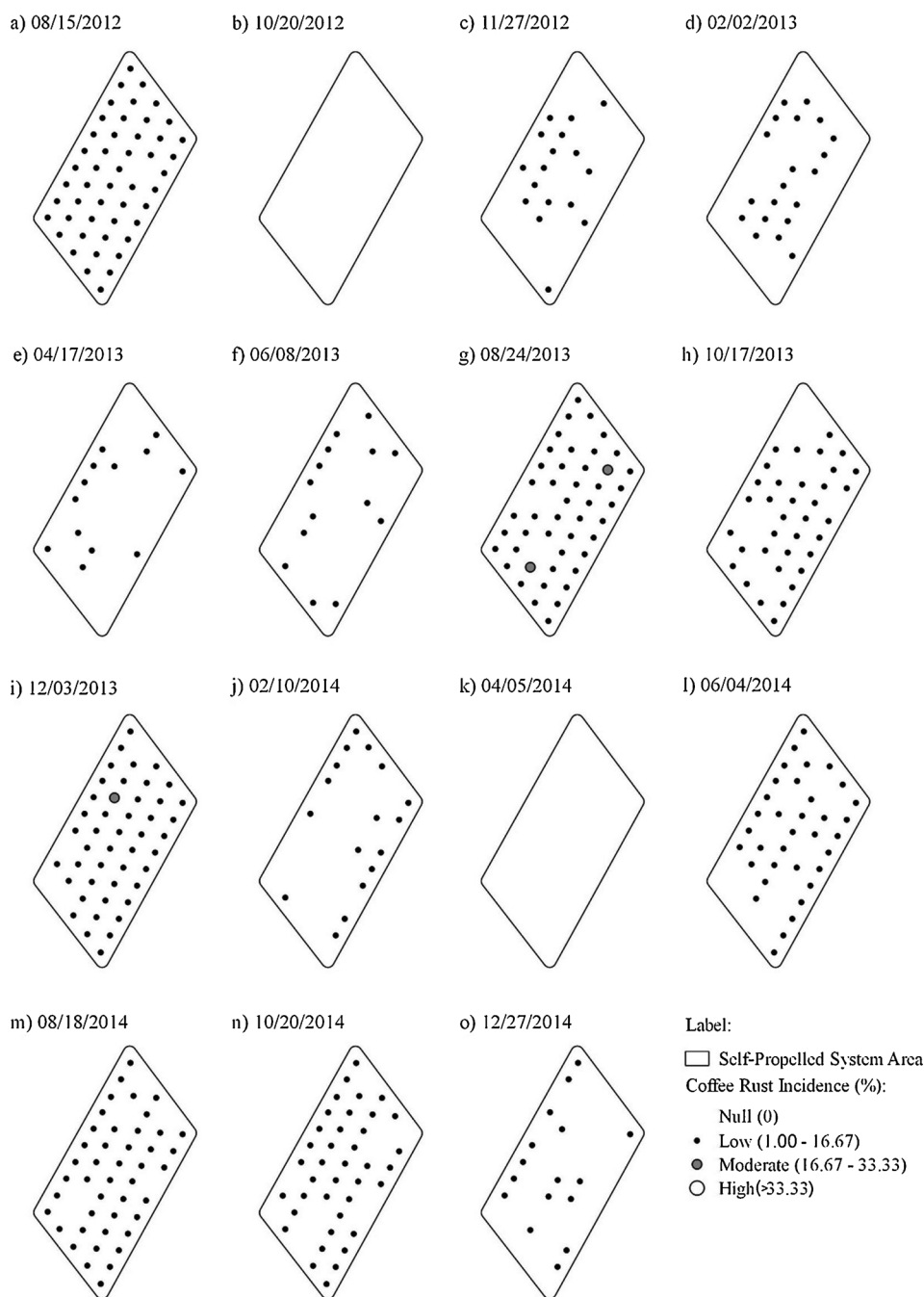
Fig. 2. Spatial distribution maps of coffee rust incidence (*Hemileia vastatrix*) in area cultivated with Acaiá 474/19 cultivar (*Coffea arabica* L.) under self-propelled irrigation system in Carmo do Rio Claro, Minas Gerais, Brazil.

growth was high in all periods, except the moderate values observed mainly in August, October and December 2013, December and June 2014 (Fig. 8).

In the cultivated area under rainfed system, the leaf growth percentage was high in November 2012, February and April 2013. In October and December 2013 the leaf growth was null due to the pruning. In February and April 2014, there was a low leaf growth, when the leaves reappeared as moderate in the aerial part of the plant in June 2014 (Fig. 9).

3.2. Temporal characterization

3.2.1. Coffee rust incidence and leaf growth

The vegetative vigor of the plant is directly associated with leaf growth, which allows to monitor the development of vegetation and the disease incidence. In this study, the reduction of the average leaf growth was observed when the incidence of rust increased in August 2013 and 2014, being the most critical period found in all evaluated areas (Fig. 10).

3.2.2. Temperature and precipitation effects in coffee rust incidence and leaf growth

Temperature values were low mainly in the months of April and June and became higher from September to March in the evaluated areas. There was difference between the evaluated sensors used to characterize the temperature, otherwise the high and low pattern of temperature along time remained the same. Temperature values near 23 °C in the months of May and June determined rust high incidence
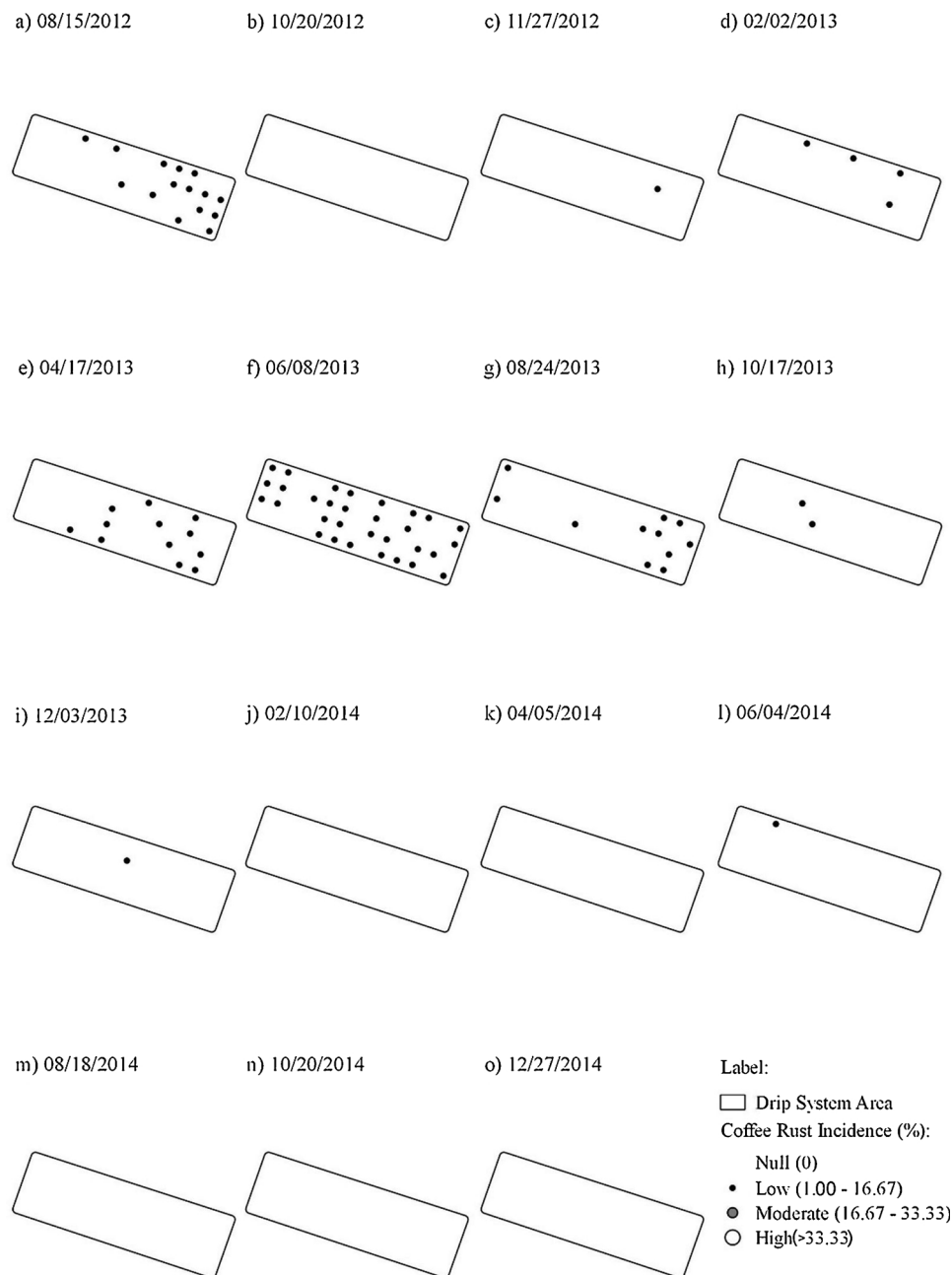
a) 08/15/2012   b) 10/20/2012   c) 11/27/2012   d) 02/02/2013

e) 04/17/2013   f) 06/08/2013   g) 08/24/2013   h) 10/17/2013

i) 12/03/2013   j) 02/10/2014   k) 04/05/2014   l) 06/04/2014

m) 08/18/2014   n) 10/20/2014   o) 12/27/2014

Label:

☐ Drip System Area
Coffee Rust Incidence (%):

   Null (0)
•   Low (1.00 - 16.67)
◉   Moderate (16.67 - 33.33)
○   High(>33.33)

Fig. 3. Spatial distribution maps of coffee rust incidence (*Hemileia vastatrix*) in area cultivated with Acaiá 474/19 cultivar (*Coffea arabica* L.) under drip irrigation system in Carmo do Rio Claro, Minas Gerais, Brazil.

values in August from 2012 to 2014 (Fig. 11).

In the short-wave infrared region, green vegetation presented low energy reflectance when compared to near infrared in all irrigated areas, except in the rainfed area. There was a significant reflectance increase in the months of November of 2013 and October 2014 in the rainfed area, possibly due to the occurrence of drought in this rainy season (Fig. 12), different from irrigated areas, which received constant water and did not present such behavior.

3.3. Spectral characterization

3.3.1. Spectral signature

There was a greater spectral (Fig. 13) and temporal variation (Fig. 10) of rust in the center pivot irrigation system when compared to the other irrigation management systems, presenting high values of average incidence of rust above 30% in the periods close to harvest,

from June to August 2013 and 2014. The highest coffee rust incidence occurred in August and corresponded to the values of lower NIR reflectance for all evaluated areas, independently of the irrigation management system. In the visible, SWIR-1 and SWIR-2 spectral regions, there were higher reflectance values in the rainfed area when compared to irrigated areas in rainy periods. High coffee rust incidence values mainly in center pivot and rainfed coffee fields determined reduction in the average reflectance of NIR and green and increase reflectance in red, SWIR-1 and SWIR-2 when compared to periods with lower rust in the coffee fields (Fig. 13).

The healthy vegetation was verified by the negative correlation between coffee rust and NIR band in the self-propelled and center pivot irrigation systems (Table 3), and by the positive correlation between leaf growth and green band in the drip irrigation system (Table 4). There was a positive correlation between leaf growth and visible region, SWIR-1 band, SWIR-2 band in the drip irrigation system. There was
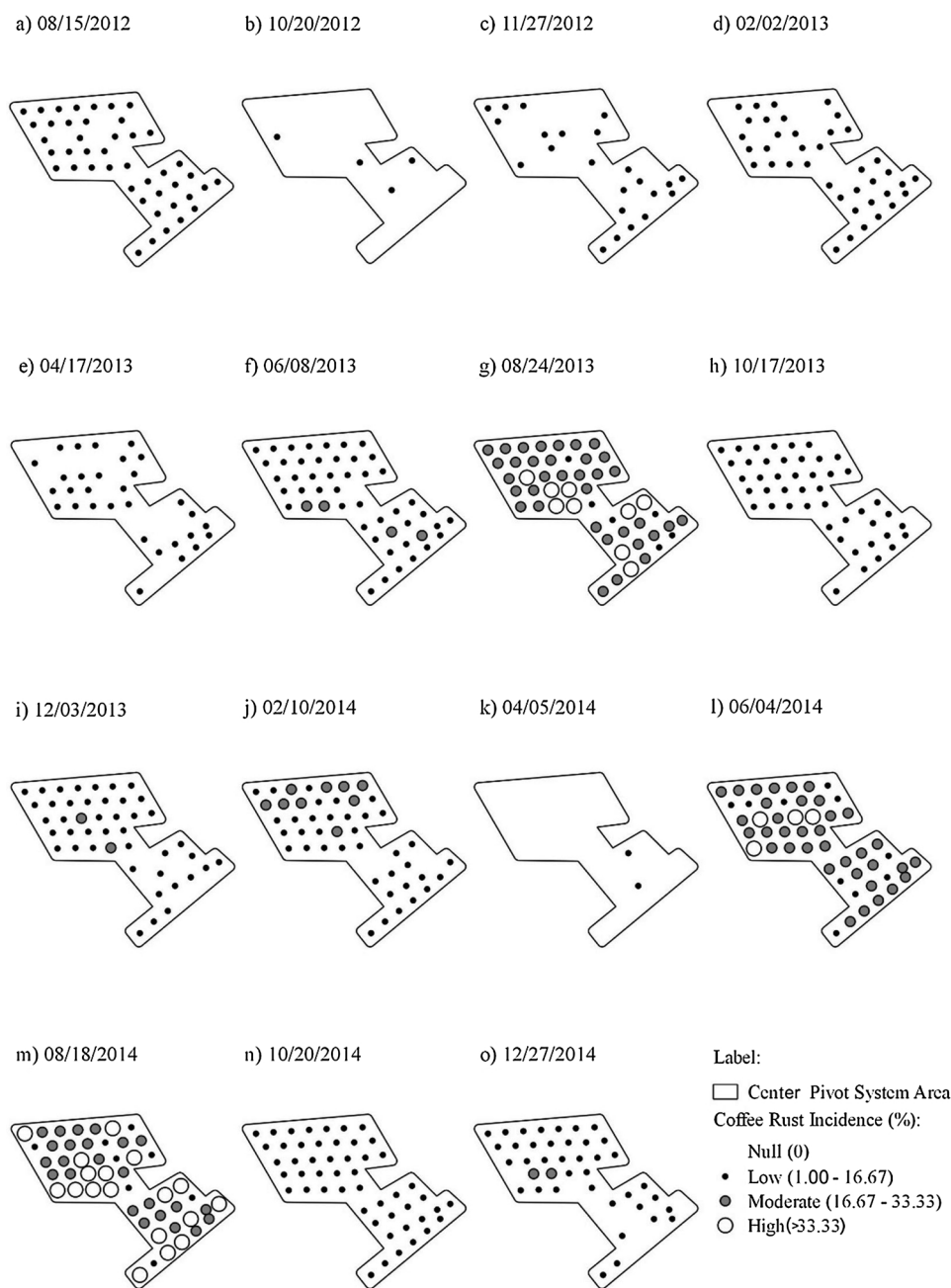
Fig. 4. Spatial distribution maps of coffee rust incidence (*Hemileia vastatrix*) in area cultivated with Acaiá 474/19 cultivar (*Coffea arabica* L.) under center pivot irrigation system in Carmo do Rio Claro, Minas Gerais, Brazil.

negative correlation between leaf growth and red band in the rainfed system (Table 4).

High coffee rust incidence values mainly in center pivot and rainfed coffee fields determined reduction in the average reflectance of NIR and green and increase reflectance in red, SWIR-1 and SWIR-2 when compared to periods with lower rust in the coffee fields.

The highest values of average coffee rust incidence were on August 24, 2013 and August 18, 2014 in all studied areas, independently of the irrigation system and corresponded to the reduction of NIR reflectance values at these dates. It was also observed a negative correlation between NIR and coffee rust, due to the increase of coffee rust incidence in the coffee leaves and the reduction of NIR reflectance in the same periods (Tables 3 and 4).

4. Discussion

4.1. Spatial characterization

4.1.1. Coffee rust incidence

The center pivot irrigation system showed the highest variation in the disease progress. This behavior may be due to the constant leaf wetness of the center pivot, which caused high rust infection and spread in the coffee leaves, determining higher incidence in comparison to the other evaluated management systems.

The highest incidence of rust varied between the months of June and August, while the highest incidence was between May and June, varying from August to September, similar as observed by Custódio et al. (2010) and Garçon et al. (2004).

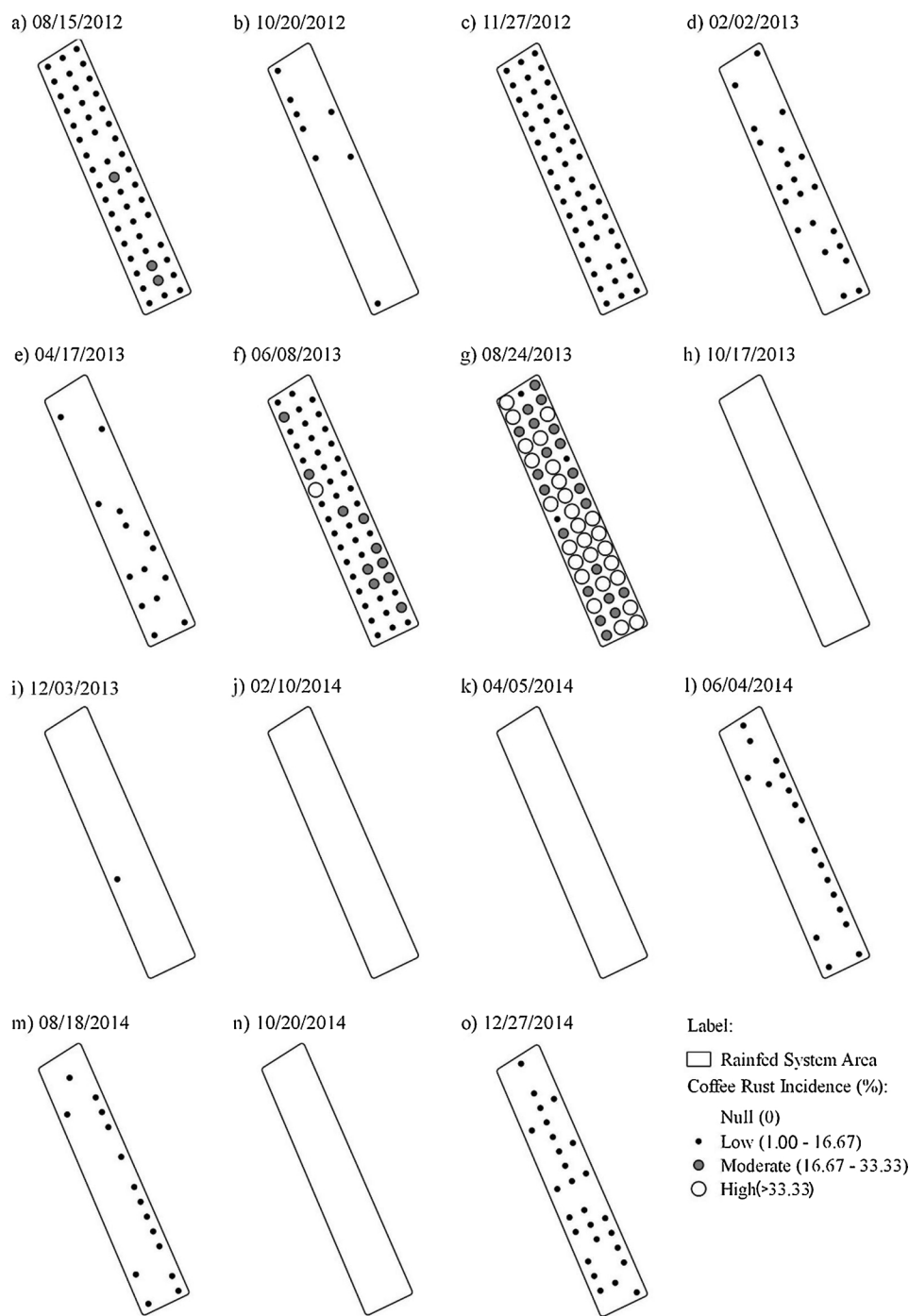In areas drip irrigated coffee field, the coffee rust incidence values

Fig. 5. Spatial distribution maps of coffee rust incidence (*Hemileia vastatrix*) in an area cultivated with Acaiá 474/19 cultivar (*Coffea arabica* L.) under rainfed system in Carmo do Rio Claro, Minas Gerais, Brazil.

observed in July and September were also observed by Talamini et al. (2003). After this period, the rate of progress became low similar as observed in this work.

It is worth noting that, although irrigation is not the only factor that will determine the increase in the coffee rust incidence, it will influence the microclimate of the crop, interacting with the soil type, amount of nutrients, factors related to crop management, cultivar, size and spacing among others coffee trees (Ribeiro do Vale, Zambolim, 1997). In addition, irrigation may confer greater resistance by increasing plant vigor (Campbell, Madden, 1990), as observed by the low rust incidence values in the field with drip irrigation or by favoring epidemics (Rotem and Palti, 1969), as observed in the coffee field with center pivot.

4.1.2. Leaf growth

The high incidence of rust associated with coffee fruit harvest probably led to a reduction in plant leaf growth in center pivot and rainfed fields. The lowest values found for average leaf growth varied between the months of June and August, as was already observed in other studies dealing with the loss associated with the disease, which can reach up to 50% of the coffee tree. The main injury to plants is the loss of leaves, responsible for reducing their photosynthetic area, with consequent death of the plagiotropic branches and reflexes on the following flowering and fruit harvest (Gree, 1993; Pozza et al., 2010).

In other crops such as rice (*Oryza sativa*) (Bastiaans and Roumen, 1993), beans (*Phaseolus vulgaris* L.) (Bassanezi et al., 2001), grapes (*Vitis*
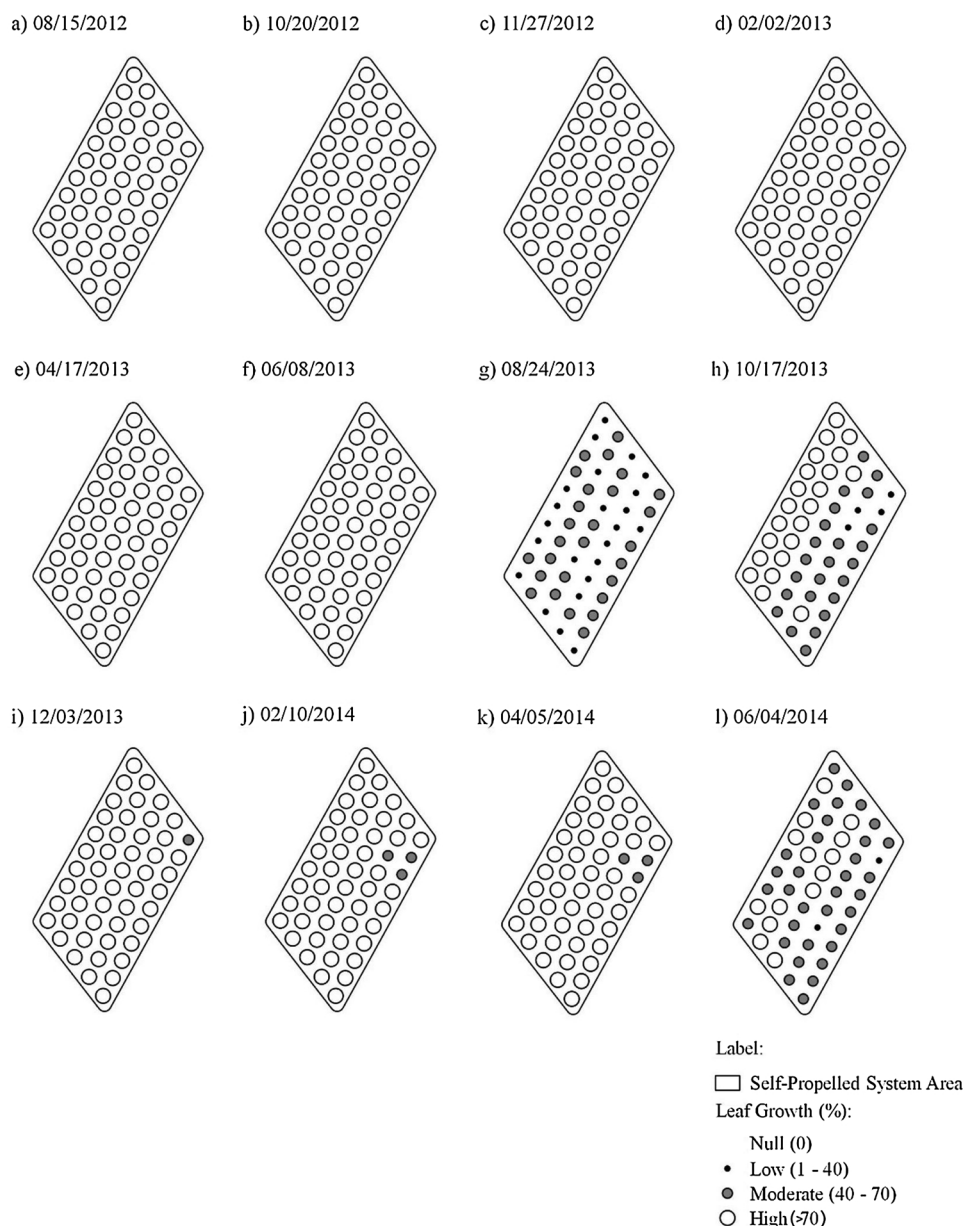
Fig. 6. Spatial distribution maps of coffee leaf growth in area cultivated with Acaiá 474/19 cultivar (*Coffea arabica* L.) under self-propelled irrigation system in Carmo do Rio Claro, Minas Gerais, Brazil.

vinifera) (Moriondo et al., 2005), wheat (*Triticum aestivum*) (Bethenod et al., 2001), sugarcane (*Saccharum* ssp. Hybrids) (Zhao et al., 2011), it has been shown that fungal infections can reduce the productivity of crops, reducing the photosynthetic efficiency of the remaining area of green leaves. The leaf area is an indicative parameter of yield, as it is important for the accomplishment of the photosynthetic process, which depends on the photosynthetic rate per unit area of the leaf and the interception of the solar radiation. These factors are influenced by the characteristics of the canopy architecture and the size of the photo-assimilator system (Favarin et al., 2002).

Another important factor that causes stomatal inhibition of photosynthesis is water stress, which can cause non-uniform closure of the stomata and may interfere with the photosynthetic capacity of the plant. A reduced capacity for photosynthesis is likely to decrease the efficiency with which the intercepted radiation is used by the plant (Lopes and Berger, 2001).

4.2. Temporal characterization

4.2.1. Coffee rust incidence, temperature, precipitation and leaf growth

The reduction of the average leaf growth was observed when the incidence of rust increased in August of 2013, being the most critical period found in all coffee fields. In the center pivot irrigation system and rainfed system, there was decrease of leaf growth in the period after the peak of rust incidence mainly in center pivot and rainfed coffee fields. Cunha et al. (2004) evaluating coffee rust control and the effects of the disease on yield and leaf growth also observed higher rust incidence values between July and August 2001 and between May and August 2002. The authors verified that was a reduction of coffee rust incidence in the second year due to the lower yield and higher leaf growth.

Factors such as large fruit load, high planting density, temperature between 21–25 °C, shading, nutritional imbalance, water deficit, high relative humidity, low luminosity and long periods of leaf wetness favor the rust progress in the field (Carvalho and Chalfoun, 1998, 1999,
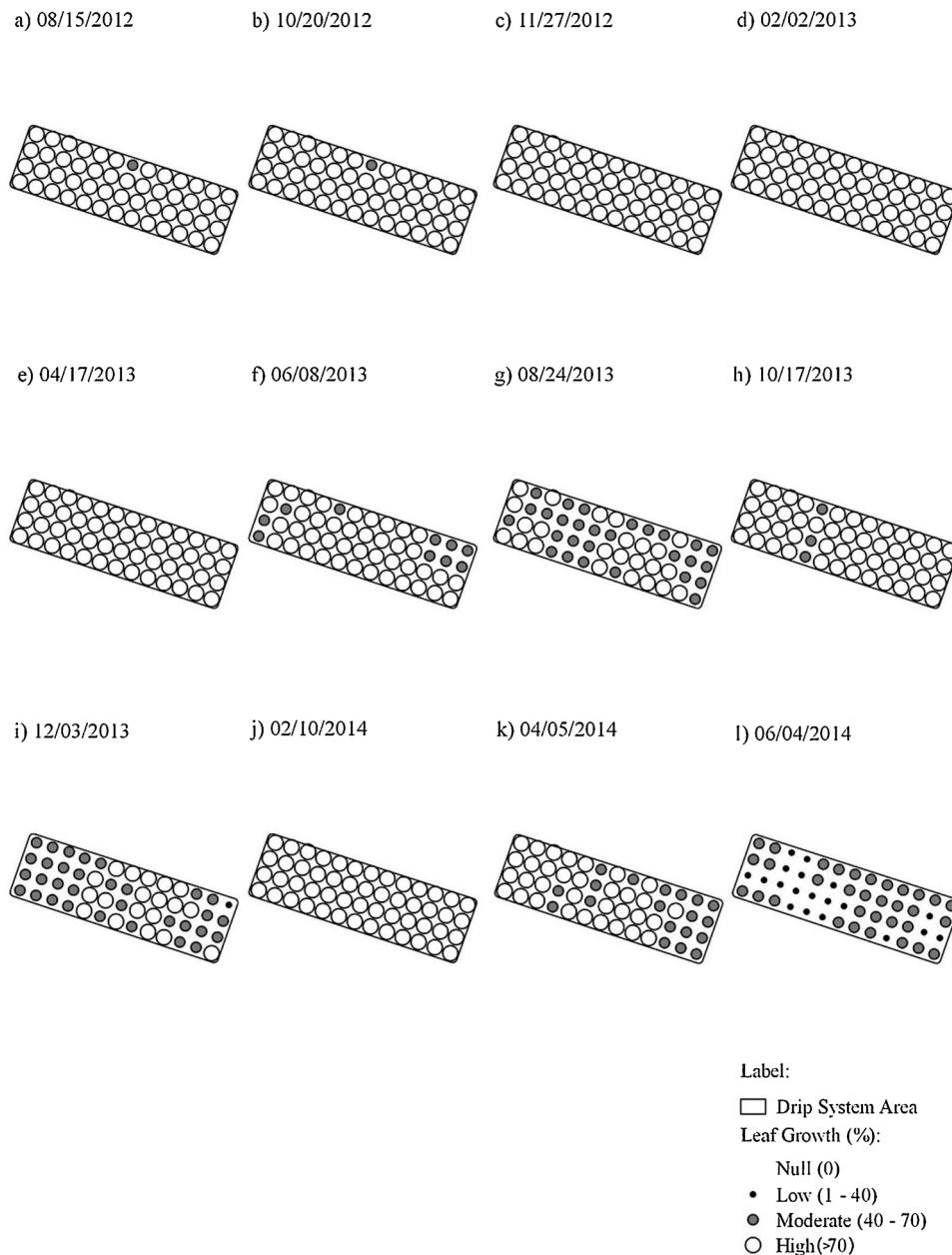
a) 08/15/2012   b) 10/20/2012   c) 11/27/2012   d) 02/02/2013

e) 04/17/2013   f) 06/08/2013   g) 08/24/2013   h) 10/17/2013

i) 12/03/2013   j) 02/10/2014   k) 04/05/2014   l) 06/04/2014

Label:

□ Drip System Area
Leaf Growth (%):

Null (0)
• Low (1 - 40)
◉ Moderate (40 - 70)
○ High (>70)

Fig. 7. Spatial distribution maps of coffee leaf growth in area cultivated with Acaiá 474/19 cultivar (*Coffea arabica* L.) under drip irrigation system in Carmo do Rio Claro, Minas Gerais, Brazil.

Pozza et al., 2010; Ward, 1882).

4.3. Spectral characterization

4.3.1. Spectral signature

The positive correlation between leaf growth and SWIR-1, SWIR-2 bands in the drip irrigation system can be related to the effects mixed objects of soil and vegetation in the image pixels considering the age of 2.5 years old of the coffee trees in the field.

The negative correlation between leaf growth and red band in the rainfed system can be related to the red light absorption by the coffee leaves for production energy by photosynthesis and causing coffee vegetation cover growth.

There was also a negative correlation between the near infrared and the coffee rust. Thus, with the increase of coffee rust incidence in the coffee tree, there was a reduction in the NIR reflectance in the field.

Chemura et al. (2016) evaluating coffee rust infection levels in plants installed in greenhouse using Sentinel-2 spectral resolution also observed high reflectance of the visible region and low reflectance of NIR as indication of stressed plants, associated with a decline in the amount and composition of leaf chlorophyll, which can be used as an initial indicator of infection and subsequent stress caused by the rust.

Reis et al. (2006), observing wheat leaf rust caused by *Puccinia triticina*, using the solar radiation reflectance readings performed by a CropScan portable multi-spectrum radiometer model MSR87, noted that 88% of the wheat yield reduction may be explained by the decrease in the reflectance of solar radiation, in the near infrared band, caused by the infection caused by the disease. The higher the severity of the disease, the higher the reflectance of the solar radiation at the wavelengths of the visible and the smaller in the near infrared wavelength.

In the near infrared region, the vegetation reflected large amount of energy. The reflected energy was well correlated with the amount of biomass produced by the plants. The main factor that controls the near infrared reflectance are the intercellular spaces present in the
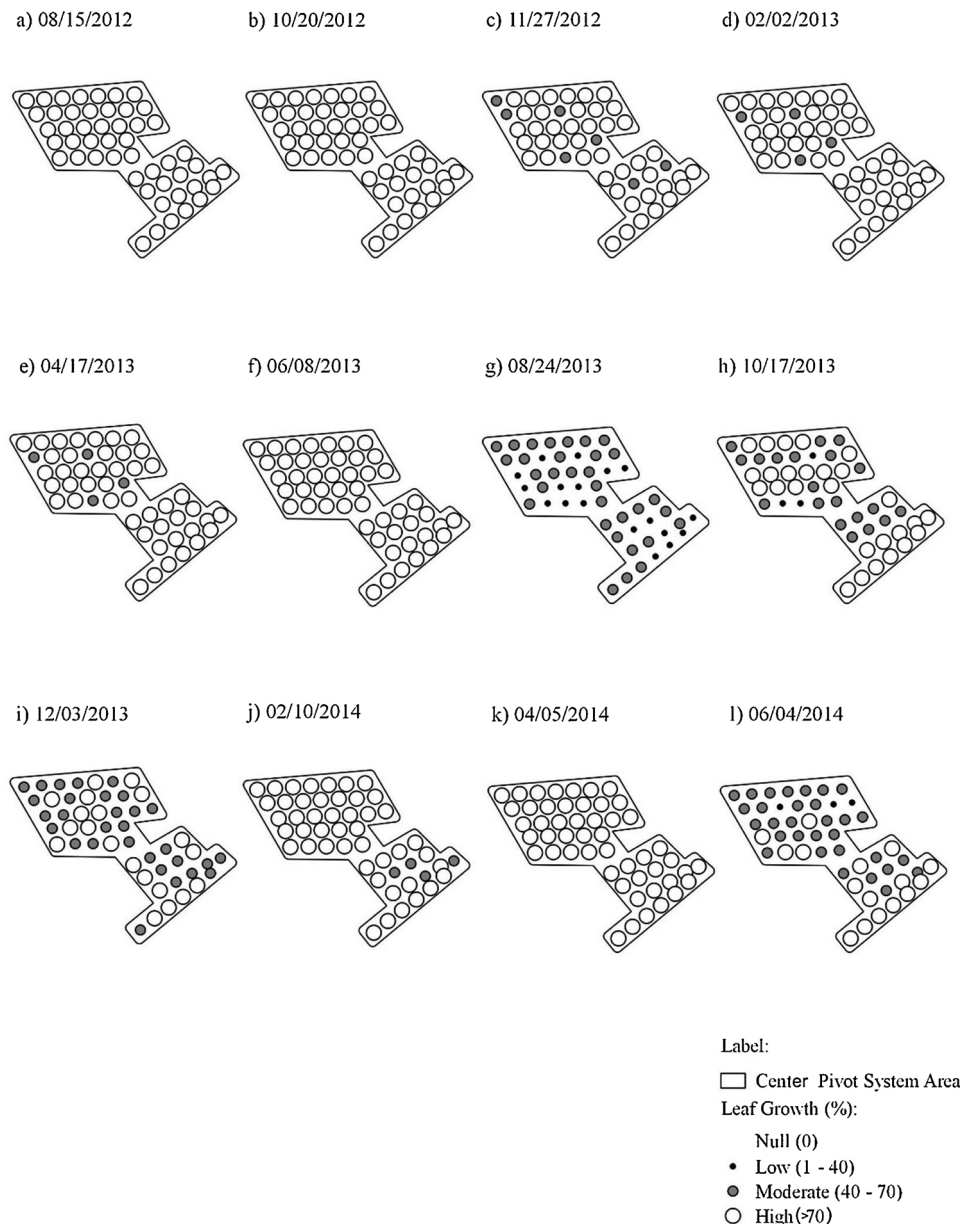
Fig. 8. Spatial distribution maps of coffee leaf growth in area cultivated with Acaiá 474/19 cultivar (*Coffea arabica* L.) under center pivot irrigation system in Carmo do Rio Claro, Minas Gerais, Brazil.

mesophyll layer. The green and healthy vegetation reflects in the region of the near infrared of 45–50% of the energy that arrives. The rest of the energy (another 45–50%) is practically transmitted to the lower or adjacent layers of the canopy (Jensen, 2009).

In the short-wave infrared region (SWIR-1 and SWIR-2), green vegetation presented lower energy reflectance when compared to near infrared in all irrigated areas, except in the rainfed area, in which there was a significant increase of SWIR reflectance in the months of November of 2013 and October 2014, possibly due to the occurrence of drought in this rainy season, different from irrigated areas, which receive constant water and did not present such behavior. This medium infrared range shows sensitivity to the water content present in the plant (Ponzoni et al., 2012; Jensen, 2009). Thus, the increase in the reflectance of the short-wave infrared occurs when the water content in the plant decreases (Novo, 2008) and can be related to the occurrence of diseases in the plant.

Short-wave infrared region was correlated with water stress in canopies of *coniferous forests* (Pierce et al., 1990) and loss of water by the

banana leaf due to the action of *Mycosphaerella fijiensis*, determining high SWIR reflectance values where the infection rate was high in the crop (Rodríguez-Gaviria and Cayón, 2008). As a result of the disease, the internal structure of the leaf undergoes alteration and may have reduced photosynthetic tissue, as well as alter the leaf spectral response in different spectral regions.

According to Naue et al. (2010), factors such as plant tissue health, after infection by phytopathogens, interfere in the quality and quantity of reflected radiation of the plants and react by altering its spectral characteristic, which allows the detection of diseases through remote sensing.

Katsuhama et al. (2018) observed that NDVI was useful to discriminate areas of coffee leaf rust infection allowing early-stage countermeasures against the infection.

Thus, coffee host spectral characteristic regionalized in the field can be detected remotely by Landsat imagery and *in situ* data collection to establish proper management at the site where the disease manifests in the plant.
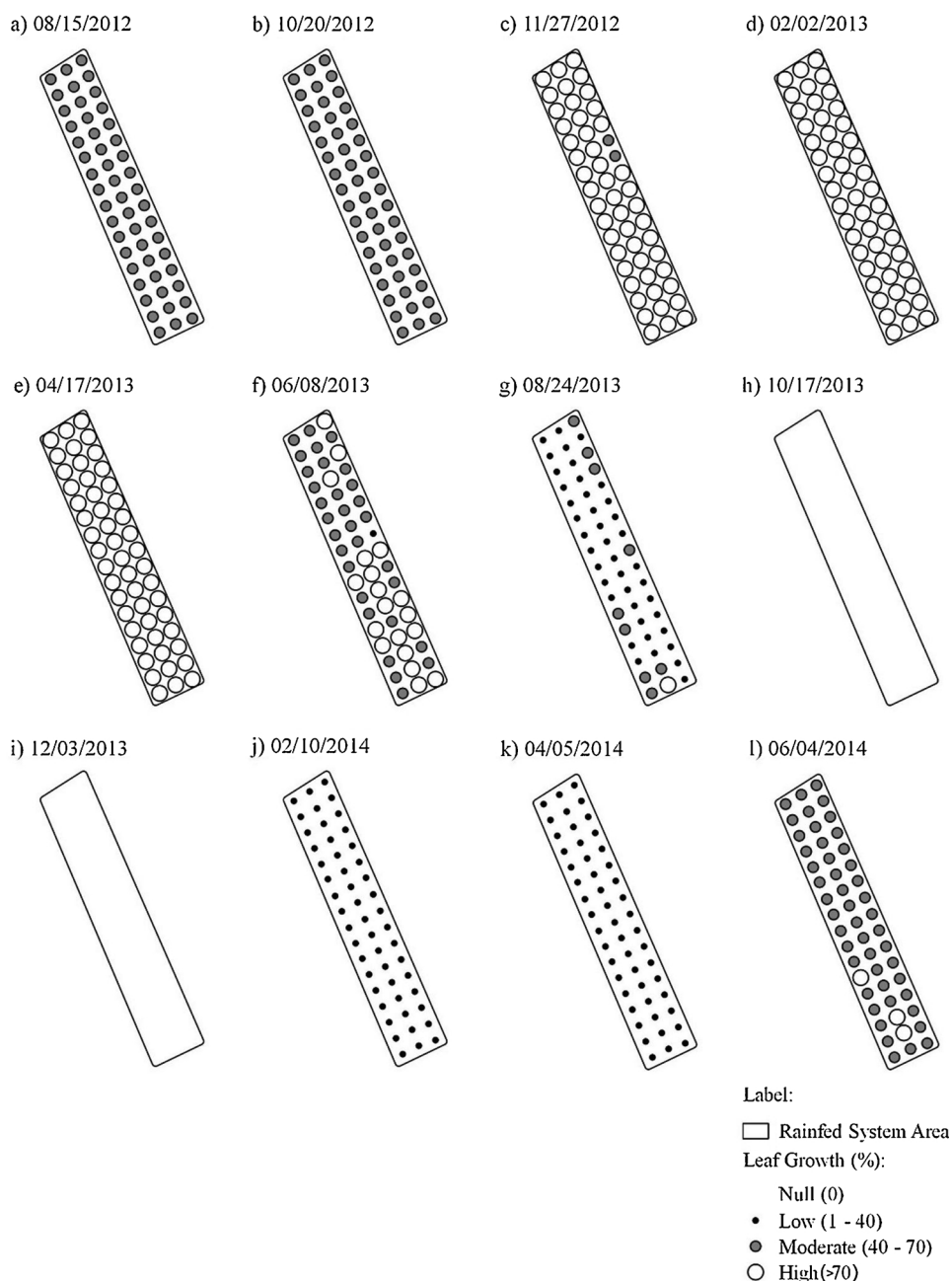
Fig. 9. Spatial distribution maps of coffee leaf growth in area cultivated with Acaiá 474/19 cultivar (*Coffea arabica* L.) under rainfed system in Carmo do Rio Claro, Minas Gerais, Brazil.

With the increased availability of free computing resources and remote sensing information available, coffee disease monitoring and forecasting systems are expected to evolve over the coming years, so that remote sensing and digital image processing will become an integral part of coffee rust integrated management systems.

5. Conclusion

The remote sensing process was an useful tool for coffee rust monitoring using Landsat imagery when associated with *in situ* data collection. There was a greater spectral and temporal variation of rust in the center pivot irrigation system when compared to the other irrigation management systems, presenting high values of average incidence in the periods close to the harvest period, from June to August 2013 and 2014.

The highest coffee rust incidence occurred in August and

corresponded to the values of lower NIR reflectance for all evaluated areas, independently of the irrigation management system. High coffee rust incidence values mainly in center pivot and rainfed coffee fields determined reduction in the average reflectance of NIR and green and increase reflectance in red, SWIR-1 and SWIR-2 when compared to periods with lower rust in the coffee fields.

Host spectral characteristic regionalized in the field must be evaluated by different sensor resolution to detect remotely the rust at moderate levels to establish the disease integrated management in the coffee agroecosystem

AUTHORSHIP STATEMENT

The authors declare that they meet authorship criteria are listed as authors, and all authors certify that they have participated sufficiently in the work to take public responsibility for the content, including
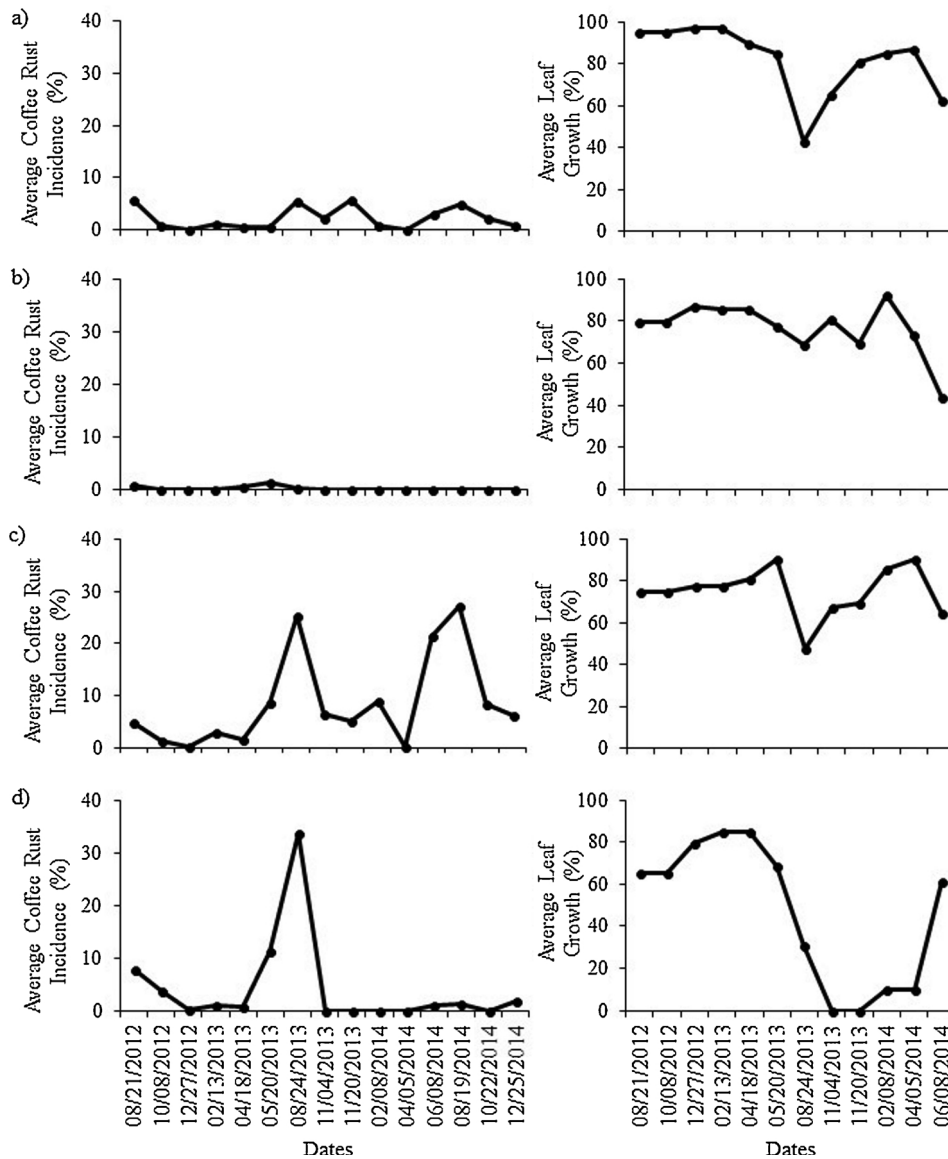
Fig. 10. Coffee rust progress curves (%) and average leaf growth curves (%) of cultivated areas under (a) self-propelled, (b) drip, (c) center pivot irrigation systems and (d) rainfed system.
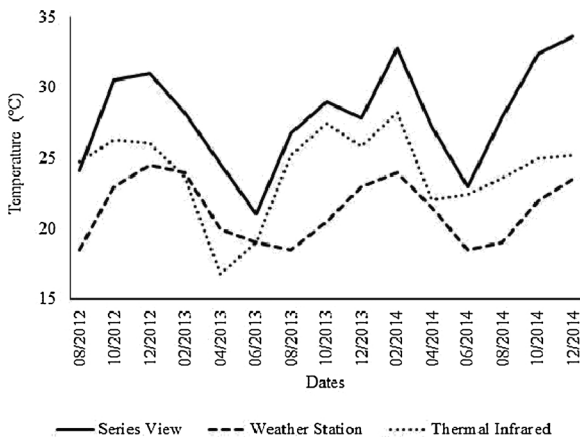

Fig. 11. Comparison of average temperature (°C) of coffee areas using data from Series View - MODIS (INPE), Weather Station in Lavras, MG, Brazil (INMET) and Thermal Infrared (Landsat-7/ETM + e Landsat-8/OLI-TIRS).
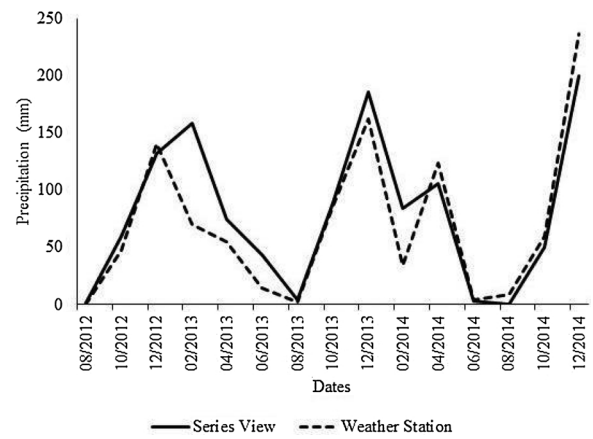
Fig. 12. Comparison of average precipitation (mm) of coffee areas using data from Series View - MODIS (INPE) and Weather Station in Lavras, MG, Brazil (INMET).
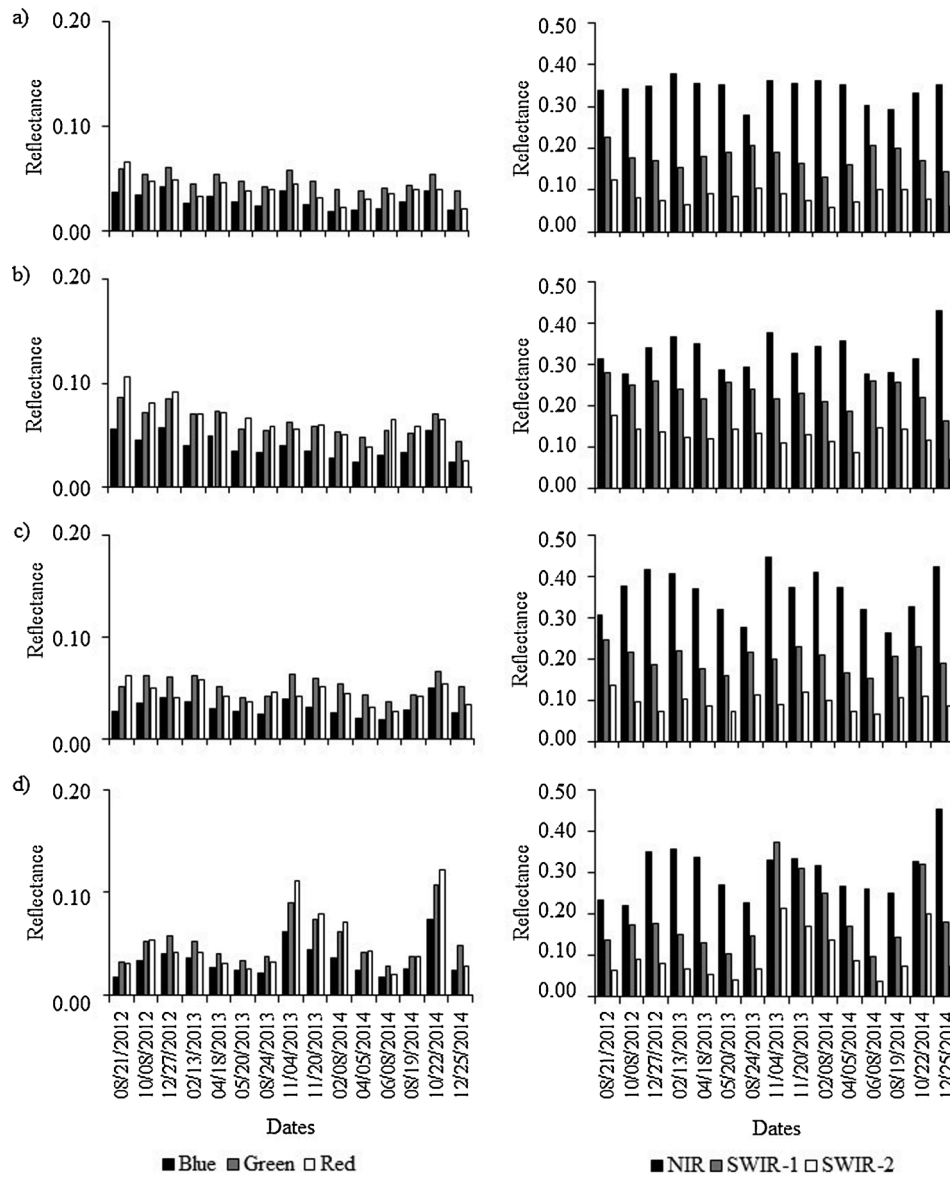
Fig. 13. Average reflectance of visible wavelengths of blue (0.45–0.52 μm), green (0.52–0.60 μm) and red (0.63–0.69 μm) (left) and near infrared (NIR) (0.77–0.90 μm) (SWIR-1) (1.57–1.75 μm) and short-wave infrared (SWIR-2) (2.08–2.35 μm) (right) of coffee fields under (a) self-propelled, (b) drip, (c) center pivot irrigation systems, and (d) rainfed system (For interpretation of the references to colour in this figure legend, the reader is referred to the web version of this article).

Table 3

Pearson correlation between the average reflectance of the blue, green, red, near infrared (NIR), short-wave infrared-1 (SWIR-1) and short-wave infrared-2 (SWIR-2) of Landsat-7 and Landsat-8 images, with average coffee rust incidence (*Hemileia vastatrix*) *in situ* data for coffee fields under self-propelled, drip, center pivot irrigation systems and rainfed system.

Study Area	Blue	Green	Red	NIR	SWIR-1	SWIR-2
Self-Propelled				− 0,617*		
Drip						
Center Pivot				− 0,559*		
Rainfed						

  * Significant correlation p $\leq$ 5%.

Table 4

Pearson correlation between the average reflectance of the blue, green, red, near infrared (NIR), short-wave infrared-1 (SWIR-1) and short-wave infrared-2 (SWIR-2) of Landsat-7 and Landsat-8 images, with average coffee leaf growth *in situ* data for coffee fields under self-propelled, drip, center pivot irrigation systems and rainfed system.

Study Area	Blue	Green	Red	NIR	SWIR-1	SWIR-2
Self-Propelled						
Drip	0,613*	0,624*	0,691*		0,656*	0,595*
Center Pivot						
Rainfed			− 0,707*			

  * Significant correlation p $\leq$ 5%.

participation in the concept, design, analysis, writing, or revision of the manuscript. Furthermore, each author certifies that this material or similar material has not been and will not be submitted to or published in any other publication before its appearance in the International Journal of Applied Earth Observation and Geoinformation.

Declaration of Competing Interest

The authors declare that they have no known competing financial interests or personal relationships that could have appeared to influence the work reported in this paper.

Acknowledgement

References

Agrios, G.N., 2005. Plant Pathology, 5th ed. Elsevier Academic Press, London, pp. 922p.

Albuquerque, M.P., Albuquerque, M.P., 2000. Processamento De Imagens: Métodos e Análises. Centro Brasileiro de Pesquisas Físicas MCT, Rio de Janeiro – Brasil, pp. 1–12.

Bassanezi, R.B., Amorim, L., Bergamin Filho, A., Hau, B., Berger, R.D., 2001. Accounting for photosynthetic efficiency of bean leaves with rust, angular leaf spot and anthracnose to assess crop damage. Plant Pathol. 50, 443–452.

Bastiaans, L., Roumen, E.C., 1993. Effect on leaf photosynthetic rate by leaf blast for rice cultivars with different types and levels of resistance. Euphytica. 66, 81–87.

Bethenod, O., Huber, L., Slimi, H., 2001. Photosynthetic response of wheat to stress induced by *Puccinia recondita* and post-infection drought. Photosynthetica. 39, 581–590.

Boechat, L.T., Pinto, F.A.C., Paula Jr., T.J., Queiroz, D.M., Teixeira, H., 2014. Detecção do mofo-branco no feijoeiro, utilizando características espectrais. Rev. Ceres 61 (6), 907–915.

Boldini, J.M., 2001. Epidemiologia da ferrugem e da cercosporiose em cafeeiro irrigado e fertirrigado. Dissertação (Mestrado Em Agronomia). Universidade Federal de Lavras, Lavras, MG 67 p.

Bravo, C., Moushou, D., West, J., McCartney, A., Ramon, H., 2003. Early disease detection in wheat fields using spectral reflectance. Biosyst. Eng. 84, 137–145.

Campbell, C.L., Madden, L.V., 1990. Introduction to Plant Disease Epidemiology. John Wiley, New York 532 p.

Carvalho, V.L., Chalfoun, S.M., 1999. Controle Da Ferrugem: a Importância Da Época De Execução. Epamig. (Circular Técnico, 104), Lavras 44 p.

Carvalho, V.L., Chalfoun, S.M., 1998. Manejo integrado das principais doenças do cafeeiro. Informe Agropecuário. 19 (193), 27–35.

Chemura, A., Mutanga, O., Dube, T., 2016. Separability of coffee leaf rust infection levels with machine learning methods at Sentinel-2 MSI spectral resolutions. Precis. Agric. 18, 859–881.

Crósta, A.P., 1992. Processamento Digital De Imagens De Sensoriamento Remoto. UNICAMP, Campinas 170p.

Cunha, R.L., Mendes, A.N.G., Chalfoun, S.M., 2004. Controle químico da ferrugem do cafeeiro (*Coffea arabica* L.) seus efeitos na produção e preservação do enfolhamento. Ciência E Agrotecnologia 28 (5), 990–996.

Custódio, A.A.P., Pozza, E.A., Custódio, A.A.P., Souza, P.A., Lima, L.A., Lima, L.M., 2010. Intensidade da ferrugem e da cercosporiose em cafeeiro quanto à face de exposição das plantas. Coffee Sci. 5 (3), 214–228.

Delalieux, S., van Aardt, J., Keulemans, W., Coppin, P., 2007. Detection of biotic stress (*Venturia inaequalis*) in apple trees using hyperspectral data: non-parametric statistical approaches and physiological implications. Eur. J. Agron. 27, 130–143.

Dhau, I., Adam, E., Mutanga, O., Ayisi, K., Abdel-Rahman, E.M., Odindi, J., Masocha, M., 2017. Testing the capability of spectral resolution of the new multispectral sensors on detecting the severity of grey leaf spot disease in maize crop. Geocarto Intenational. 2, 1–14.

Favarin, J.L., Neto, D.D., García, A.G., Nova, N.A.V., Favarin, M.G.G.V., 2002. Equações para a estimativa do índice de área foliar do cafeeiro. Pesquisa Agropecuária Brasileira, Brasília 37 (6), 769–773.

Florenzano, T.G., 2011. Iniciação Em Sensoriamento Remoto, 3rd ed. Oficina de Textos, São Paulo 128 p. amp. e atual.

Garçon, C.L.P., Zambolim, L., Mizubuti, E.S.G., Vale, F.X.R., Costa, H., 2004. Controle da ferrugem do cafeeiro com base no valor de severidade. Fitopatol. Bras. 29 (5), 486–491.

Gree, G., 1993. Epidemiology of Coffee Leaf Rust in the Eastern Highlands. Newsletter - Coffee Research Institute, pp. 16–20 2(9).

Guimarães, P.T.G., Garcia, A.W.R., Alvarez, V.H.A., Prezotti, L.C., Viana, A.S., Miguel, A.E., Malavolta, E., Corrêa, J.B., Lopes, A.S., Nogueira, F.D., Monteiro, A.V.C., Oliveira, J.A., 1999. Cafeeiro. In: Ribeiro, A.C., Guimarães, P.T.G., Alvarez, V.H.A. (Eds.), Recomendações para o uso de corretivos e fertilizantes em Minas Gerais (pp. 289-302). Comissão de Fertilidade do Solo do Estado de Minas Gerais (CFSEMG), Viçosa 5 ª Aproximação Cafeeiro.

Hillnhütter, C., Mahlein, A.K., Sikora, R.A., Oerke, E.C., 2012. Use of imaging spectroscopy to discriminate symptoms caused by *Heterodera schachtii* and *Rhizoctonia solani* on sugar beet. Precis. Agric. 13, 17–32.

Huerta, S.A., 1963. Par de folhas representativo del estado nutricional del cafeto. Cenicafé. 14 (1), 11–127.

Instituto Brasileiro de Geografia e Estatística (IBGE), 2010. IBGE Cidades@|Minas Gerais: Carmo Do Rio Claro. Available in: http://cidades.ibge.gov.br/xtras/perfil.php?lang=&codmun=311440&search=minas-gerais|carmo-do-rio-claro. Accessed in: Feb. 2016 Disponível em.

Instituto Nacional De Meteorologia (INMET), 2016. Rede De Estações: Estações Automáticas – Machado/MG. Disponível em:. http://www.inmet.gov.br/portal/index.php?r=estacoes/.

Jensen, J.R., 2009. Sensoriamento remoto do ambiente: uma perspectiva em recursos terrestres. In: Epiphanio (coordenador), JoséCarlos N., Formaggio, Antonio R., Santos, Athos R., Rudorff, Bernardo F.T., Almeida, Cláudia M., Galvão, L.ênio S. (Eds.), Tradução Da 2ª Ed. Por (Pesquisadores Do INPE). São José dos Campos, Parêntese 672 p.

Katsuhama, N., Imai, M., Naruse, N., Takahashi, Y., 2018. Discrimination of areas infected with coffee leaf rust using a vegetation index. Remote. Sens. Lett. 9 (12), 1186–1194.

Kobayashi, T., Kanda, E., Kitada, K., Ishiguro, K., Torigoe, Y., 2001. Detection of rice panicle blast with multispectral radiometer and the potential of using airborne multispectral scanners. Phytopathology. 91, 316–323.

Kottek, M., Grieser, J., Beck, C., Rudolf, B., Rubel, F., 2006. World Map of the Köppen-Geiger climate classification updated. Meteorol. Z. 15 (3), 259–263.

Liu, W.T.H., 2006. Aplicações de sensoriamento remoto. Campo Grande, Ed. UNIDERP. 908 p. Lopes, D.B., Berger, R.D. 2001. The Effects of Rust and Anthracnose on the Photosynthetic Competence of Diseased Bean Leaves. Phytopathology. 91 (2), 212–220.

Lopes, D.B., Berger, R.D., 2001. The effects of Rust and Anthracnose on the photosynthetic competence of diseased bean leaves. Phytopathology 91, 212–220.

Mahlein, A.K., Rumpf, T., Welke, P., Dehn, H.W., Plümer, L., Steiner, U., Oerke, E.C., 2013. Development of spectral indices for detecting and identifying plant diseases. Remote Sens. Environ. 128, 21–30.

Mahlein, A.K., Steiner, U., Dehne, H.W., Oerke, E.C., 2010. Spectral signatures of sugar beet leaves for the detection and differentiation of diseases. Precis. Agric. 11, 413–431.

Marques Filho, O., Neto, H.V., 1999. Processamento Digital De Imagens. Rio de Janeiro, Brasport 331 p.

Ministério da Agricultura, 2016. Pecuária E Abastecimento (MAPA). Vegetal: Culturas – Café. Disponível em: < http://www.agricultura.gov.br/vegetal/culturas/cafe/saiba-mais > . Acesso em: 10 mar. 2016.

Moriondo, M., Orlandini, S., Giuntoli, A., Bindi, M., 2005. The effect of downy and powdery mildew on grapevine (*Vitis vinifera* L.) leaf gas exchange. J. Phytopathol. 153, 350–357.

Mutanga, O., Dube, T., Galal, O., 2017. Remote sensing of crop health for food security in Africa: potentials and constraints. Remote. Sens. Appl. Soc. Environ. 8, 231–239.

Naue, C.R., Marques, M.W., Lima, N.B., Galvíncio, J.D., 2010. Sensoriamento remoto como ferramenta aos estudos de doenças de plantas agrícolas: uma revisão. Rev. Bras. Geogr. Fãsica 3, 190–195.

Novo, E.M.L.M., 2008. Sensoriamento Remoto: Princípios E Aplicações, 3rd ed. Edgard Blücher, São Paulo.

Pierce, L.L., Running, S.W., Riggs, G.A., 1990. Remote detection of canopy water stress in coniferous forests using NS001 Thematic Mapping Simulation and Thermal Infrared Multispectral Scanner. Photogramm. Eng. Remote Sensing 56 (5), 579–586.

Ponzoni, F.J., Shimabukuro, Y.E., Kuplich, T.M., 2012. Sensoriamento Remoto Da Vegetação. 2ª Edição Atulizada E Ampliada. Oficina de Textos, São Paulo 177 p.

Pozza, E.A., Carvalho, V.L., Chalfoun, S.M., 2010. Sintomas de injúrias causadas por doenças em cafeeiro. In: Guimaraes, R.J., Mendes, A.N.G., Baliza, D.P. (Eds.), Semiologia do cafeeiro: sintomas de desordens nutricionais, fitossanitárias e fisiológicas semiologia do cafeeiro. Ed. UFLA., Lavras, pp. 68–106.

Reis, E.M., Leites, A., Forcelini, C.A., 2006. Relações entre intensidade da ferrugem da folha, refletância da radiação solar e rendimento de grãos na cultura do trigo Embrapa 16. Fitopatol. Bras. 31, 447–454.

Ribeiro Do Vale, F.X., Zambolim, L., 1997. Controle de doenças de plantas: grandes culturas Vol. 2. Departamento de Fitopatologia, Viçosa, pp. 83–179.

Rodrigues, S., Filho, G.S.F., Almeida, W.A., Neto, A.F.C., 2010. Desenvolvimento do café arábica (*Coffea arabica*) submetido a diferentes lâminas de irrigação, nas condições do estado de Rondônia. Glob. Sci. Technol. 3 (1), 44–49.

Rodríguez-Gaviria, A.A., Cayón, G., 2008. Efecto de *Mycosphaerella fijiensis* sobre la fisiología de la hoja de banana. Agron. Colomb. 26 (2), 256–265.

Rotem, J., Palti, J., 1969. Irrigation and Plant Diseases. Annual Review of Phytopathology. 7, 267-288. Silva, A.J. da., Canteri, M.G., Santiago, D.C., Hikishima, M., Silva, A.L. 2009. A reflectância na estimativa do efeito de fungicidas no controle da ferrugem asiática da soja. Summa Phytopathol. 35 (1), 53–56.

Talamini, V., Pozza, E.A.A., Souza, P.E., Silva, A.M., 2003. Progresso da ferrugem e da cercosporiose em cafeeiro (*Coffea arabica* L.) com diferentes épocas de início e parcelamentos da fertirrigação. Ciência e Agrotecnologia. 27 (1), 141–149.

Tyagi, P., Bhosle, U., 2014. Radiometric correction of multispectral images using radon transform. J. Indian Soc. Remote. Sens. 42 (1), 23–34.

United States Geological Survey (USGS). 2016. Available in: < http://landsat.usgs.gov/ > . Acess in: feb. 2016.

Vermote, E.F., Tanre, D., Deuze, J.L., Herman, M., Morcrette, J.J., 1997. Second simulation of the satellite signal in the solar spectrum, 6S: an overview. IEEE Trans. Geosci. Remote. Sens. 35, 675–686.

Waller, J.M., 1982. Coffee rust-epidemiology and control. Crop. Prot. 1 (4), 385–404.

Ward, H.M., 1882. Research on the life history of *Hemileia vastatrix*, the fungus of the coffee leaf disease. J. Linnean Soc. (Botany) 12 (3), 299–335.

Webb, K.M., Calderón, F.J., 2015. Mid-infrared (MIR) and near-infrared (NIR) detection of *rhizoctonia solani* AG-2-2 IIIB on barley-based artificial inoculum. Appl. Spectrosc. 69 (10), 1129–1136.

Zhang, M., Qin, Z., Liu, X., Ustin, S., 2003. Detection of stress in tomatoes induced by late blight disease in California, USA, using hyperspectral remote sensing. Int. J. Appl. Earth Obs. Geoinf. 4, 295–310.

Zhao, D., Glynn, N.C., Glaz, B., Comstock, J.C., Sood, S., 2011. Orange rust effects on leaf photosynthesis and related characters of sugarcane. Plant Dis. 95, 640–647.